Colliders and Collider Physics at the Highest Energies
Muon Colliders at 10 GeV to 100 TeV
HEMC'99 Workshop, Montauk, New York 1999
Editor B.J. King, AIP Conference Proceedings Vol.530, 2000. pp. 38-47.

Fringe Field Effects in Muon Rings

Martin Berz, Kyoko Makino and Béla Erdélyi

Abstract. Because of the predominance of large emittances, muon storage rings have a tendency to being rather sensitive to nonlinear effects. In this paper we study the effects of the nonlinearities due to the lattice elements' fringe fields, which have a fundamentally different behavior from normal multipole terms. It is found that for given scenarios for lattices and emittances, the fringe field effects have dramatic influences on the dynamics and stability of particles and hence require careful study of correction options.

FRINGE FIELD EFFECTS IN BEAM DYNAMICS

The nonlinearities due to fringe fields are a well-known phenomenon in the field of high resolution particle spectrographs [1,2]. In large hadron storage rings, their effects frequently are negligible, but they have a tendency to become noticeable in rings of smaller radius, particularly at larger emittances. In order to understand the fringe effects, we expand the r and ϕ dependencies of the scalar potential in Taylor and Fourier series and have

$$V = \sum_{k=0}^{\infty} \sum_{l=0}^{\infty} M_{k,l}(s) \cos(l\phi + \theta_{k,l})\, r^k. \tag{1}$$

In cylindrical coordinates, the Laplace equation has the form

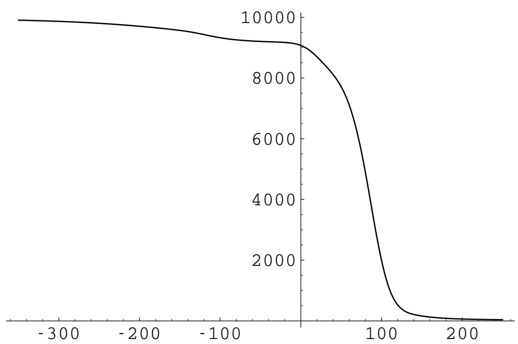

FIGURE 1. The fringe field of an LHC quadrupole.

$$\Delta V = \frac{1}{r}\frac{\partial}{\partial r}\left(\frac{r\partial V}{\partial r}\right) + \frac{1}{r^2}\frac{\partial^2 V}{\partial \phi^2} + \frac{\partial^2 V}{\partial s^2} = 0; \tag{2}$$

inserting the Fourier–Taylor expansion of the potential, we obtain [3]

$$\Delta V = \sum_{k,l=0}^{\infty} \left\{ M_{k,l}(s)\cos\left(l\phi + \theta_{k,l}\right)\left(k^2 - l^2\right) + M''_{k-2,l}(s)\cos\left(l\phi + \theta_{k-2,l}\right) \right\} r^{k-2}, \tag{3}$$

where the convention has been used that all coefficients $M_{k,l}$ vanish for negative indices. In case $M_{k,l}$ is constant, we obtain that $k = l$, and hence the radial and angular dependencies are coupled in the well-known way. However, in case $M_{k,l}$

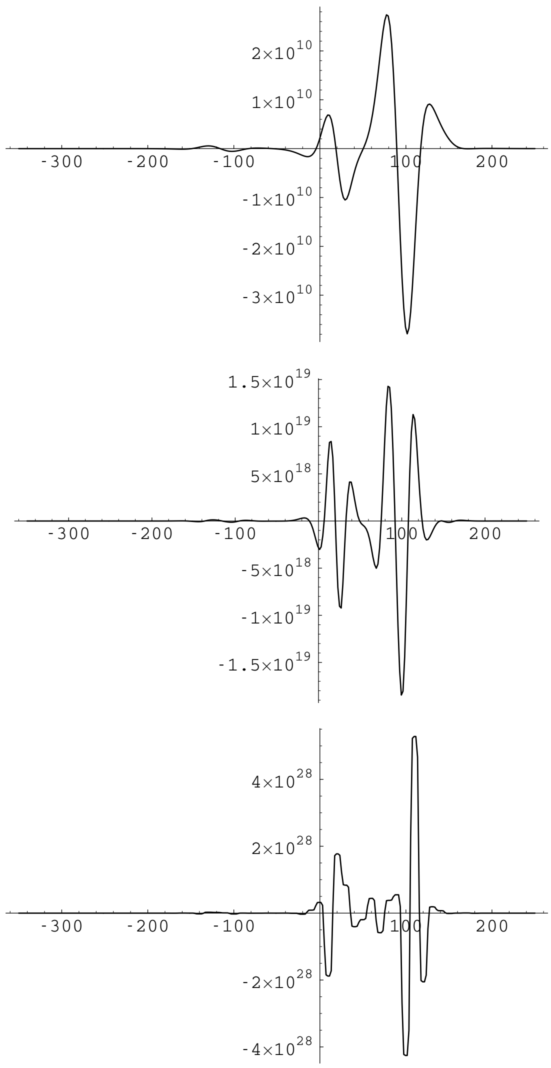

FIGURE 2. The s-derivatives of the quadrupole strength of orders 4, 8, and 12 at the fringing region of an LHC quadrupole.

is not constant, besides the terms $M_{l,l}$, there are also the terms $M_{l+2,l}$, $M_{l+4,l}$, ... which introduce higher-order radial dependencies to a given angular dependence. Specifically, we have

$$M_{l+2n,l}(s) = \frac{M_{l,l}^{(2n)}(s)}{\prod_{\nu=1}^{n}\left((l)^2 - (l+2\nu)^2\right)}, \quad \text{and} \quad \theta_{l,l} = \theta_{l+2,l}, \theta_{l+4,l}, \ldots \tag{4}$$

where $M_{l,l}^{(2n)}$ is the $2n$th derivative of $M_{l,l}$. In practice this entails that fringe field effects become more and more relevant the more the particles are away from the axis of the element, which of course is directly connected to the emittance of the beam.

The additional non-multipole nonlinearities of the fringe fields couple to higher derivatives of the multipole strength. These derivatives can assume rather striking forms; as an example we show the value of the quadrupole strength as well its derivatives of orders 4, 8,and 12 for an LHC quadrupole from the final focus section in Figure 1 and Figure 2.

The fringe field effects can be particularly easily studied in the map picture using differential algebraic methods [3]. Their complete treatment to any order is possible in the code COSY INFINITY [4–6].

FRINGE FIELD EFFECTS IN MUON STORAGE RINGS

In the following we present observations related to fringe field effects. Similar to the situation in the study of kinematic correction [7], we limit ourselves to the mere observation of the effects, without attempting to devise strategies for their correction through nonlinear elements, which of course should also include the influence of all other relevant nonlinear effects.

The consequences of the fringe field effects influence all orders of the motion, beginning from the linear behavior. The linear effects even affect the tune, and it turned out that for the lattices in question, the effects are significant. However, since the comparison of nonlinear motion is most relevant for the situation where the tunes are identical, in practice a re-fitting of the linear layout back to the original tune is appropriate. To simplify this procedure, COSY has a mode that automatically adds linear correction elements such that the linear map of the system with fringe fields is the same as without fringe fields. This mode was used throughout for the subsequent studies.

Furthermore, the detailed shape of the fringe field fall off influences the details of the nonlinear behavior, yet information of the fall off is not known until the actual mechanical design of the elements. Thus we assumed a default fall off that describes the situation in many multipoles with benign end field design [6].

As a first example, we study the effects on a 30 GeV neutrino factory ring and a 30 GeV Higgs factory ring kindly supplied by Carol Johnstone [8]. The neutrino

TABLE 1. The beginning part of the Taylor transfer map of a 30 GeV neutrino factory ring without fringe field effects.

Expansion coefficients of x,a,y,b depending on the exponents of xayb				
(x,	(a,	(y,	(b,	xayb
-0.1936744	0.1416905	0	0	1000
-6.792904	-0.1936744	0	0	0100
0	0	0.1961760	-0.2456274E-01	0010
0	0	39.14526	0.1961760	0001
0.9450713E-01	0.3330788E-02	0	0	2000
0.1377180	-0.5612056E-01	0	0	1100
-0.5801038	-0.6286416	0	0	0200
0	0	0.1229122	-0.3076403E-03	1010
0	0	0.6994628	0.2591721E-02	0110
0	0	-0.4902813	-0.1229122	1001
0	0	4.130383	-0.6994626	0101
-0.8336143E-02	-0.1539706E-02	0	0	0020
0.2386714	0.1206977E-01	0	0	0011
13.28519	2.453805	0	0	0002
11.55775	-0.1950424	0	0	3000
-81.95874	4.704898	0	0	2100
392.7585	-40.95482	0	0	1200
-1667.934	610.1026	0	0	0300
0	0	-0.7719322	-0.4832862E-01	2010
0	0	14.24336	0.4605147	1110
0	0	-417.3649	-2.944554	0210
0	0	-6.277132	-8.007910	2001
0	0	354.6553	34.10640	1101
0	0	-782.7162	-69.64528	0201
0.2344129	-0.2585728E-01	0	0	1020
-3.593587	1.490467	0	0	0120
26.50950	-1.496885	0	0	1011
-116.8393	6.467636	0	0	0111
2245.991	-29.01786	0	0	1002
-4789.016	244.2371	0	0	0102
0	0	-1.130680	-0.7756062E-02	0030
0	0	-6.403961	-0.4518258	0021
0	0	-430.3112	-29.87579	0012
0	0	-1116.550	-1705.361	0003
-1.322453	-0.9516536E-01	0	0	4000
....	....	....	....	....

TABLE 2. The beginning part of the Taylor transfer map of a 30 GeV neutrino factory ring with fringe field effects.

Expansion coefficients of x,a,y,b depending on the exponents of xayb				
(x,	(a,	(y,	(b,	xayb
-0.1936744	0.1416905	0	0	1000
-6.792904	-0.1936744	0	0	0100
0	0	0.1961760	-0.2456274E-01	0010
0	0	39.14526	0.1961760	0001
0.9450668E-01	0.3330792E-02	0	0	2000
0.1377195	-0.5612046E-01	0	0	1100
-0.5800990	-0.6286441	0	0	0200
0	0	0.9402828	0.2251288E-01	1010
0	0	-11.70894	-0.1896604	0110
0	0	16.57293	1.476914	1001
0	0	-139.6185	-8.654864	0101
-0.1248983	0.2034706E-01	0	0	0020
-5.726400	0.5915340	0	0	0011
-215.4763	16.77799	0	0	0002
478.5009	-5.828819	0	0	3000
-2963.906	119.4893	0	0	2100
11370.25	-1164.119	0	0	1200
-57663.58	24785.65	0	0	0300
0	0	-44.02904	-7.722130	2010
0	0	1084.027	32.25581	1110
0	0	-61208.70	-414.5974	0210
0	0	-2410.660	-1200.200	2001
0	0	9632.604	4243.860	1101
0	0	-128922.6	-5760.175	0201
20.86897	-1.837551	0	0	1020
-418.5652	221.3400	0	0	0120
4203.500	-36.84456	0	0	1011
-8816.418	1001.507	0	0	0111
331876.4	-2632.727	0	0	1002
-596393.2	12424.07	0	0	0102
0	0	-94.33547	-0.6567247	0030
0	0	-681.4684	-25.23468	0021
0	0	-13103.20	-2736.609	0012
0	0	-292594.6	-141126.2	0003
-56.81891	-3.180838	0	0	4000
....	....	....	....	....

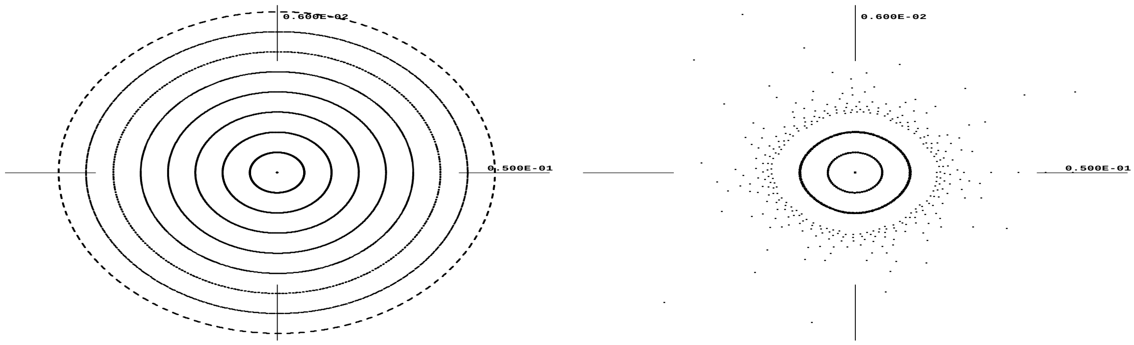

FIGURE 3. Tracking pictures for 1000 turns in a 30 GeV neutrino factory ring without (left) and with (right) fringe field effects in the same scale of 50mm×6mrad. In the absence of fringe field effects, particles seem to survive up to 100mm×15mrad with kinematic correction. With fringe field effects, only those up to 10mm×1.5mrad survive.

factory ring consists of bending elements and quadrupoles, and the Higgs factory ring furthermore has sextupoles. The full gap size of the magnets is assumed to be 10cm for the both rings.

The kinematic correction is included by default [7] in the following results. Tables 1 and 2 show the beginning part of high order Taylor transfer maps of the neutrino factory ring. Table 1 shows the case without fringe field effects, and Table 2 the case with fringe field effects. Because of the re-fitting of the linear behavior, effects can be observed from second order; overall, the nonlinearities are significantly larger than before.

The size of the dynamic aperture was estimated by tracking particles for 1000 turns with transfer maps up to 7th order. In case of no fringe field effects, particles

TABLE 3. Amplitude dependent tune shifts.

Fringe field effects		off	on	Order	Exponents	
					x	y
30 GeV neutrino factory ring	x motion	0.718979	0.718979	0	0	0
		12.0363	469.397	2	2	0
		5.32077	741.941	2	0	2
	y motion	0.218573	0.218573	0	0	0
		5.32077	741.941	2	2	0
		5.92760	472.150	2	0	2
30 GeV Higgs factory ring	x motion	0.864288	0.864288	0	0	0
		35.8432	855.939	2	2	0
		42.0333	2226.02	2	0	2
	y motion	0.665356	0.665356	0	0	0
		42.0333	2226.02	2	2	0
		422.116	4180.00	2	0	2

with x up to 1000mm and a up to 150mrad are stable without kinematic correction and those with x up to 100mm and a up to 15mrad are stable with kinematic correction in the neutrino factory ring [7]. However when the fringe field effects are included, the particles with x up to 10mm and a up to 1.5mrad survive. Figure 3 illustrates the stability of particles in case the fringe fields are on (right side) as compared to off (left side).

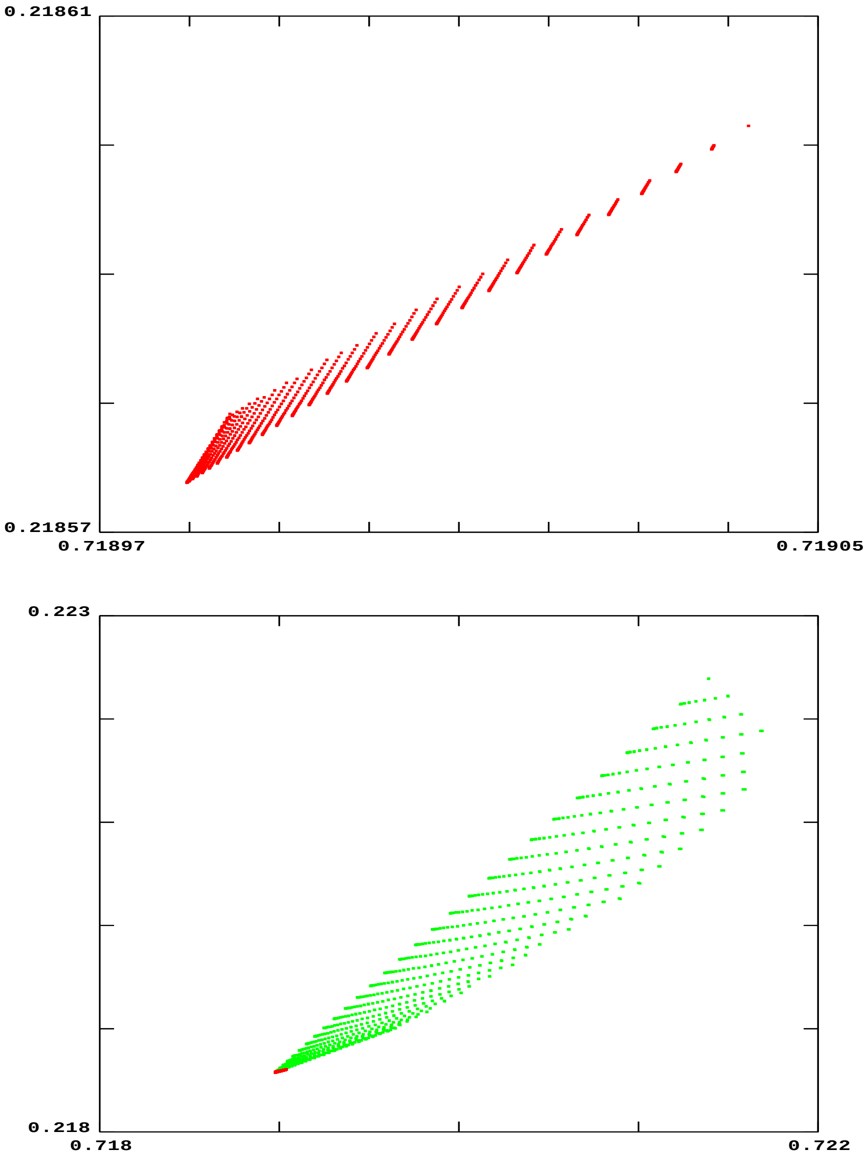

FIGURE 4. Tune footprints of a 30 GeV neutrino factory ring without (upper) and with fringe field effects. The lower picture shows both in the same scale, where the one without fringe field effects is the tiny bar at the lower left.

Based on normal form methods, amplitude dependent tune shifts were computed using COSY INFINITY [9,10]. The results with and without fringe field effects are summarized in Table 3. Figure 4 shows tune footprints of the neutrino factory ring for particles up to 6mm in radius in both x and y directions. The horizontal axis shows the x tune and the vertical shows the y tune. The upper picture shows the tune footprint without fringe field effects, and the lower shows the situation with fringe field effects. The one without fringe field effects occupies a rather small region, and it is shown as a tiny bar at the lower left in the lower picture for comparison.

Altogether, for the design of the neutrino factory ring used in the study, the dynamic aperture decreased by a factor of around 100 in x-a, and there is a large increase by a factor of around 10000 in the tune footprint area.

The 30 GeV Higgs factory ring was studied in the similar way. The tracking pictures in Figure 5 can be used to estimate the size of the dynamic aperture, and a decrease by a factor of 100 in x-a is observed due to fringe field effects. The amplitude dependent tune shifts are listed in Table 3. Figure 6 shows the tune footprints for particles up to 0.5mm in radius in both x and y directions. The upper left picture shows the situation without fringe field effects, and the upper right picture contains fringe field effects. To illustrate the difference of the size more clearly, the lower picture shows the two footprints in the same scale; the small triangle at the lower left is the tune footprint without fringe field effects. An increase of the tune footprint area by a factor of about 400 is observed.

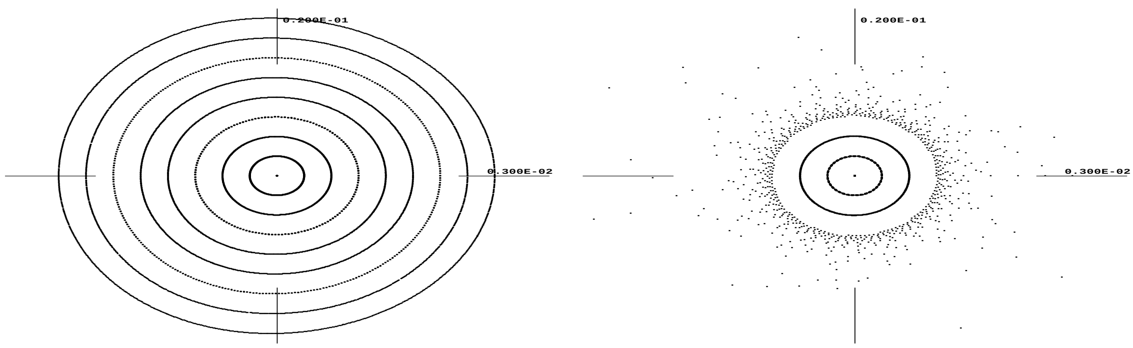

FIGURE 5. Tracking pictures for 1000 turns in a 30 GeV Higgs factory ring without (left) and with (right) fringe field effects in the same scale of 3mm×20mrad. In the absence of fringe field effects, particles seem to survive up to 6mm×50mrad with kinematic correction. With fringe field effects, only those up to 0.6mm×5mrad survive.

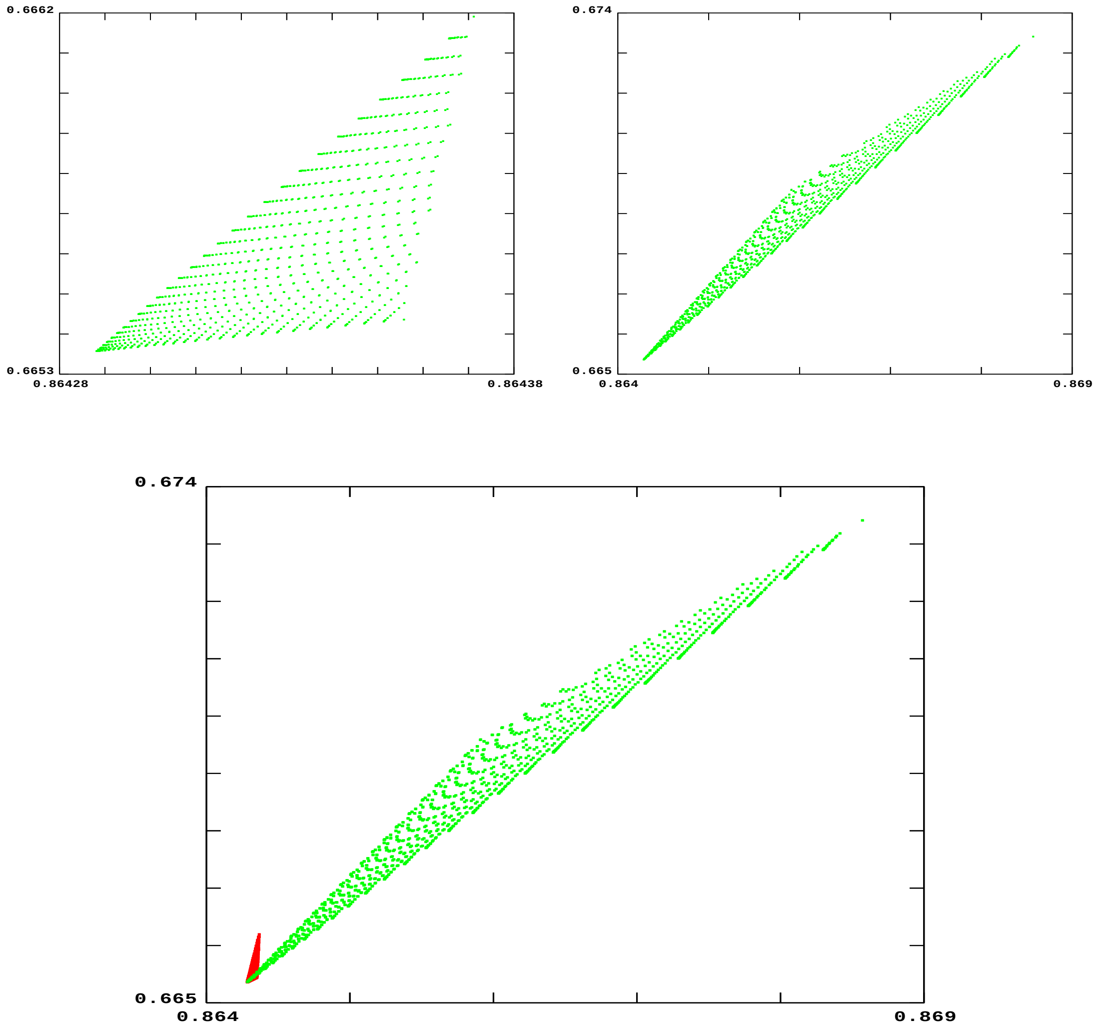

FIGURE 6. Tune footprints of a 30 GeV Higgs factory ring without (upper left) and with (upper right) fringe field effects. The lower picture shows both in the same scale, where the one without fringe field effects is the small triangle at the lower left.

ACKNOWLEDGMENTS

We thank C. Johnstone and W. Wan for providing the storage ring designs for the study. The work was supported by the US Department of Energy and the Alfred P. Sloan Foundation.

REFERENCES

1. N. Anantaraman and B. Sherrill, Editors. Proceedings of the international conference on heavy ion research with magnetic spectrographs. Technical Report MSUCL-685, National Superconducting Cyclotron Laboratory, 1989.
2. M. Berz, K. Joh, J. A. Nolen, B. M. Sherrill, and A. F. Zeller. Reconstructive correction of aberrations in nuclear particle spectrographs. *Physical Review C*, 47,2:537, 1993.
3. M. Berz. *Modern Map Methods in Particle Beam Physics*, volume 108 of *Advances in Imaging and Electron Physics*. Academic Press, San Diego, CA, 1999.
4. M. Berz et al. The COSY INFINITY web page. http://cosy.nscl.msu.edu.
5. K. Makino and M. Berz. COSY INFINITY version 8. *Nuclear Instruments and Methods*, A427:338, 1999.
6. M. Berz. COSY INFINITY Version 8 reference manual. Technical Report MSUCL-1088, National Superconducting Cyclotron Laboratory, Michigan State University, East Lansing, MI 48824, 1997.
7. K. Makino and M. Berz. Effects of kinematic correction on the dynamics in muon rings. In these proceedings.
8. Carol Johnstone. Private communication.
9. M. Berz. *High-Order Computation and Normal Form Analysis of Repetitive Systems, in: M. Month (Ed), Physics of Particle Accelerators*, volume AIP 249, page 456. American Institute of Physics, 1991.
10. M. Berz. Differential algebraic formulation of normal form theory. In *M. Berz, S. Martin and K. Ziegler (Eds.), Proc. Nonlinear Effects in Accelerators*, page 77. IOP Publishing, 1992.